

Development of Measurement Techniques for Studying Propeller Erosion Damage in Severe Wake Fields

Woody Pfitsch, Scott Gowing, David Fry, Martin Donnelly, and Stuart Jessup

Naval Surface Warfare Center, Carderock Division(NSWCCD)
9500 MacArthur Boulevard
West Bethesda, MD 20817

ABSTRACT

Preliminary propeller erosion tests have been conducted at the Naval Surface Warfare Center Carderock Division 24 inch variable pressure water tunnel (VPWT), shown in Figure 1, to establish testing procedures for evaluating various coatings to minimize cavitation erosion damage to marine propellers. A severe wake field was produced using a two dimensional, thick foil ahead of a downstream driven propeller model. This approach was derived from similar tests conducted by Miller [11]. Conventional cavitation viewing was performed with cameras viewing through the tunnel side window. Images were acquired using high speed (up to 6000 fps) and high resolution (2K x 2K) cameras. In addition, a waterproof camera was mounted inside the foil looking directly downstream at the suction face of the blade. Two propellers were tested, a 16 inch (0.406 m) diameter propeller 5388 and a 12 inch (0.305 m) diameter propeller 4119 [8]. The foil wake field was measured with LDV surveys. Accelerometers were mounted in the water tunnel test section to measure acoustic emissions of cavitation activity.

Cavitation erosion was observed at the tip of the 16 inch diameter propeller due to excessive tip vortex, and complicated vortex collapse. Moderate erosion was also observed at the inner radii, where leading edge sheet cavitation collapsed. Scanning techniques for quantifying propeller erosion damage were evaluated. These studies will transition to the 36-inch VPWT where a number of geosym propellers of different materials and coating will be assessed in a similar wake field.

INTRODUCTION

Cavitation erosion damage on marine propellers results in performance loss, noise, vibration and significant repair or replacement costs. Recently, high performance propeller coatings have been developed that have the potential to mitigate cavitation erosion damage and extend the repair cycle of ships and reduce service costs. The Naval Surface Warfare Center, Carderock Division (NSWCCD), with funding from the Office of the Secretary of Defense (OSD) Quick Reaction Funds (QRF) program has begun a program to evaluate the performance of a propeller coating, Nickel Boron (NiB), and a surface hardening method, Low Temperature Colossal Super-Saturation (LTCSS), for carburization of austenitic stainless steels [4]. This program is being managed by the Office of Naval Research (ONR). Four phases of water tunnel testing are planned for evaluation of these coatings: development of cavitation erosion measurement methods, propeller powering

and cavitation performance assessment for coated versus uncoated propellers, and evaluation of coatings erosion resistance. This paper briefly discusses the results of the first phase of testing, conducted in February – March, 2009.

Prior to this study there have been many attempts at quantifying the erosive damage caused by cavitation [1, 3, 5, 10, 11, 12, 13] including measuring mass loss of specimens subjected to cavitation collapse [1, 10] and using high speed video to document cavitation collapse [3, 12]. The approach typically used at NSWCCD at present is observation of pitting on an anodized aluminum model propeller. Erosion rates are not predicted, but the pitting observed is correlated with specific types of cavitation, which then serves as an indicator of probable erosion issues. Subsequent propeller re-design or limitation of operating conditions can then be used to avoid erosion issues in fleet use. The goal of the cavitation erosion measurement development test in this program is to incorporate and improve on some of these methods to study cavitation erosion damage on model scale propellers while taking advantage of recently developed technologies. In this test, three measurement techniques were utilized: cavitation imaging, quantitative measurements of acoustic emissions, and scanning of cavitation erosion damage to quantify material loss. In addition, the ability to generate erosive cavitation conditions in a severe wake field was evaluated. The results of these tests were used to develop testing techniques for quantifying the erosion performance of the high performance propeller coatings to be tested in phase four of testing in August – October, 2009.

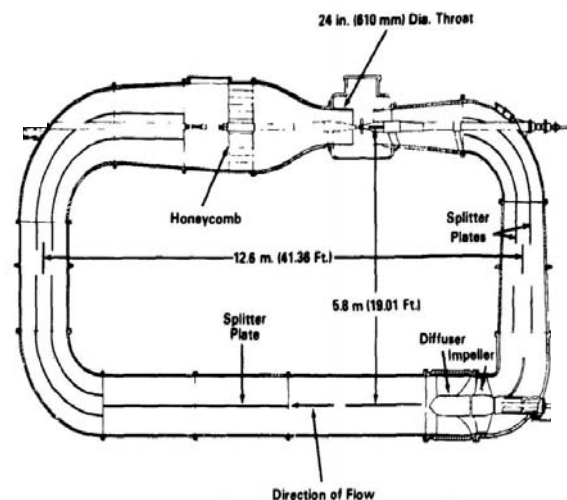


Figure 1 : 24 inch Variable Pressure Water Tunnel

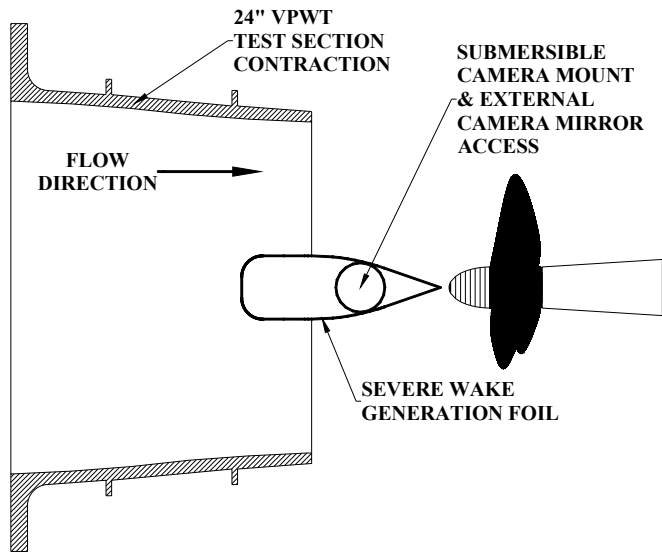


Figure 2: 24 Inch VPWT severe wake field setup

EXPERIMENTAL SET UP

Water Tunnel

This test was performed in the David Taylor 24 inch Variable Pressure Water Tunnel (24-in. VPWT) at NSWCCD. This tunnel is a vertical loop, re-circulating design with upstream and downstream propeller drives and a test speed capability of 30 knots (15.4 m/s). The tunnel is shown in Figure 1. The test was performed in the 24 inch (0.610 m) diameter open-jet test section using the 150 HP (112 kW) downstream drive to power the propeller. The static pressure in the test section can be varied from vacuum to 1 atm (101 kPa) positive pressure to model various cavitation conditions.

Tunnel velocity, test section pressure, and propeller rpm were recorded for all conditions. The reference velocity was measured by a Pitot-static probe measurement located on the tunnel center line directly below the propeller, and tunnel static pressure was measured from the static port of the same Pitot-static probe. Both pressure measurements were made using 20 psi (138 kPa) Validyne pressure transducers low-pass filtered at 10 Hz. Propeller rpm was measured using the propeller drive motor encoder.

Wake Generator

To study erosion, a scheme was needed to create a consistent, high-intensity cavitation collapse on the mid-blade region of the test propeller. This was accomplished by operating the propeller in a severe wake field. The wake was generated using a strut installed in the test section contraction immediately upstream of the propeller, with the tail end of the strut 0.72 inches upstream of the propeller fairwater (Figure 2). The strut design used a blunt front face with wire grills attached to the sides to create a large velocity defect, and the geometry was based on studies of propeller erosion performed by Miller and Dahmer [5, 11]. These studies used a similar strut to generate wakes over 40 degrees of the propeller disc with peak wake deficits of 60%.

Wake Measurement

Prior to propeller installation, the wake field was surveyed using a laser Doppler velocimetry (LDV) system as shown in Figure 3. The LDV system consisted of a TSI model 9832 fiber optic 3.25 inch (82.6 mm) diameter probe mounted rigidly to a motorized traverse which could translate the measurement point vertically and transversely across the test section. The traverse system was manually re-located at four transverse planes axially separated by 0.984 inches (25mm). The probe utilized the green (514.5nm) and blue (488nm) colors of an argon ion laser to measure axial and vertical velocity components respectively. The fiber optic probe was translated within a 12 inch (305 mm) diameter insert mounted in a test section window. The insert allowed the probe to be positioned to within 13.8 inches (350 mm) of the tunnel centerline.

Most measurements were made with a 470 mm (in water) lens that could measure one side of the test section and up to ~2.75 inches (70 mm) past the tunnel centerline. The measurement volume was 0.003 by 0.051 inches (0.07 by 1.3 mm). A second longer focal length lens allowed measurements transversely across the entire test section. This measurement volume was 0.004 by 0.075 inches (0.10 by 1.9 mm). The window insert limited the vertical range of measurements to +/- 3.93 inches (100 mm) above and below the tunnel centerline.

Doppler signals were analyzed with a TSI Model IFA 655 Digital Burst Correlator. Velocity measurements were collected over a 15 second period in non-coincident mode. Total measurements at each location varied by position and velocity component, but generally ranged between 5,000 and 50,000. The flow was seeded with silver coated glass spheres with a size range between 2 and 10 microns and a specific gravity of 2.8.

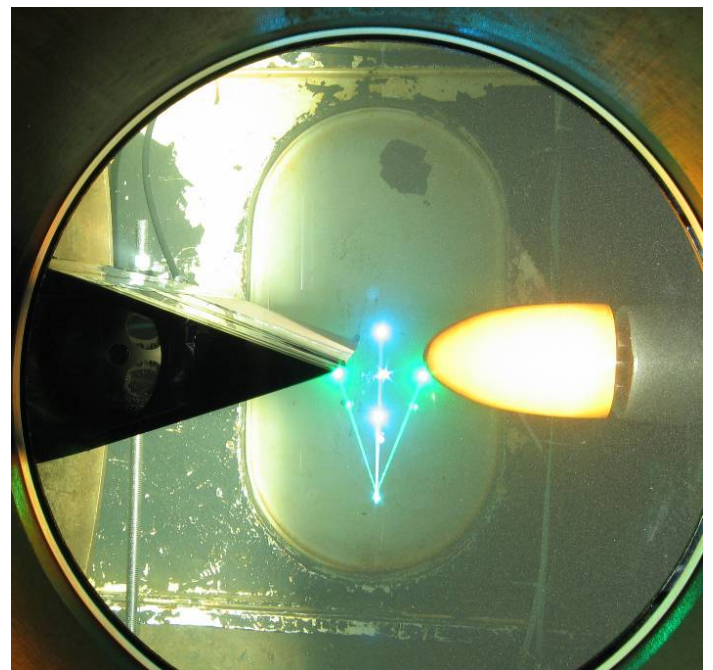


Figure 3: LDV survey of strut wake field

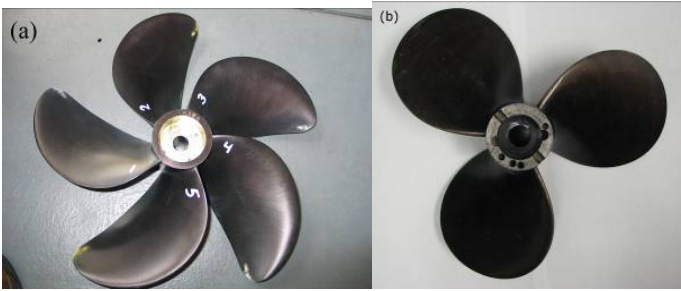


Figure 4: (a) Propeller 5388, 16-inch and (b) Propeller 4119, 12-inch propeller

Propellers

Two propellers were used to facilitate the evaluation of cavitation conditions. The first was a 16 inch (0.406 m) diameter, 5-bladed propeller, no. 5388, with a blade design identical to the propellers to be tested in the coating evaluation. This propeller is typical of naval fixed pitch propellers. Although the blade geometry of this propeller was the same as to be tested in the coatings tests, its size was overly large in the 24 in VPWT and it suffered wall effects that altered the cavitation pattern from an unblocked condition. Hence a second propeller was tested with a 12 inch (0.305 m) diameter. This 3-bladed propeller, no. 4119 [8] had a propeller/jet diameter ratio closer to that of the coating evaluation propellers to be tested in the 36-inch VPWT. Pictures of the propellers are in Figure 4. The 16 inch propeller was used extensively for most aspects of this test while the 12 inch propeller was used to study how the cavitation conditions would change with a smaller propeller and less wall effects.

Imaging

The blade sheet cavitation was viewed with a submersible Inuktun Spectrum 90 pipe inspection camera (Figure 5) mounted inside the wake generation foil immediately upstream of the propeller. Plastic windows contoured to the foil trailing edge allowed a direct view of the propeller blade as it passed through the foil's wake. This installation is shown in Figure 6. This camera system had remote pan and tilt capability, allowing the camera view to sweep radially and tangentially relative to the propeller. Images were acquired at 30 frames per second with a pixel resolution of 320 x 240 and recorded on a mini-DV tape recorder. Although this camera system has an internal incandescent light source, a strobe light system was set up to trigger off of a one-pulse per revolution signal, syncing the strobe flashes with the propeller rotation. Some frames were lit by the strobe and some were dark using this lighting scheme with the camera at 30 frames per second. The dark frames were digitally removed after acquisition to obtain continuous frame sequences with the propeller motion "frozen" by the strobe light. This camera view showed the overall extent of sheet cavitation as well as its variability from one blade passage to the next.

To capture the collapse of the cavitation and obtain high resolution images, two external camera systems were used to acquire images through windows in the tunnel. These systems will be referred to as the high-speed (HS) and high-resolution (HR) systems, respectively.



Figure 5: Submersible Camera

The HS system camera lens was focused through a hole in the wake-generating foil onto a small mirror mounted to the head of the Inuktun submersible camera. Using the pan and tilt control of that system, the mirror could be adjusted to provide a direct view of the propeller blade with the same aspect as the submersible camera (see Figure 7). This provided a direct view of the collapse region of the blade's sheet cavity. The HS imaging system was a Photron camera system with frame rates up to 6000 fps and pixel resolutions up to 1K x 1K. This high frame rate showed the development of a single cavitation event and details of the collapse of cavitation bubbles on the blade surface. The lighting for the HS system was provided by five submersible flood lights and two externally mounted photography flood lights. The lighting requirements were even more demanding because the lens was zoomed to spread the image reflected from the small mirror over the entire image sensor.

The HR imaging system was a Boulder Imaging acquisition system connected to a Pulnix camera with a pixel resolution of 2K x 2K. The frame rate of this camera was controlled by triggers from the propeller shaft one-pulse per revolution signal, effectively syncing the strobe light and camera to the propeller blade position. With this acquisition capability, every frame acquired was lit by the strobe light and no post processing was necessary to obtain continuous sequences. This system was primarily used to view the propeller from a side angle through the tunnel window.

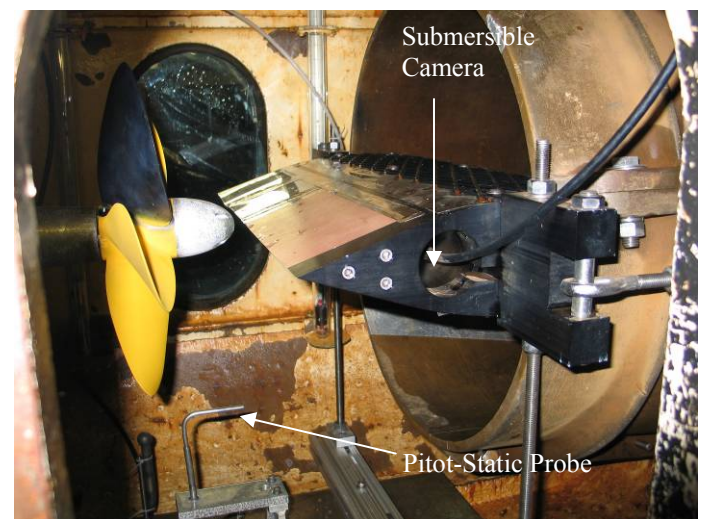


Figure 6: Wake generation foil with submersible camera



Figure 7: High speed imaging setup

Inks

To facilitate visualization of the area where cavitation erosion would occur, the 16 inch propeller blades were coated with stencil ink. The area where the ink was removed gave an indication of where blade erosion damage would occur after extended operation. Two ink types were evaluated; brush-on Marsh Rolmark white stencil ink and spray-on Diagraph Quick-Spray yellow marking ink. The condition of the stencil ink was recorded at regular intervals in the propeller operation with the submersible camera.

Acoustic Sensing

Three accelerometers were mounted in the 24 inch VPWT test section to measure the acoustic emission of cavitation. Wilcoxon Research Model 754 submersible accelerometers, with a resonance frequency of 50 kHz and a nominal sensitivity of 10 mV/g, were mounted (1) on the floor of the test section directly below the propeller, (2) under the capture nozzle of the test section, and (3) on the downstream propeller shaft strut. The accelerometer signals were conditioned with a PCB Model 482A20 Signal Conditioner, and the data were acquired with a Tektronix DPO-4034 oscilloscope at a 500 kHz sampling rate in sample lengths of 0.2 seconds. Thirty two samples were acquired at random intervals at each condition.

Erosion Damage Evaluation

To determine the loss of propeller material, a Keyence LJ-G030 2D laser displacement sensor [9] was planned to be used to measure surface elevation contours. This sensor uses a fan-shaped laser beam to scan a surface and output elevation coordinates of the surface normal to the sensor axis (normal to

the surface) with a repeatability of 1 μm . Two methods were planned for use of this sensor. The first was to scan the entire propeller using a 6 degree-of-freedom traverse system to hold the Keyence sensor normal to the blade and automate the scanning process. Comparison of scans made before and after cavitation erosion indicates the amount of material loss. The second method would scan positive molds of the eroded areas using Flexbar ReproRubber model #16131 casting material [6]. This simpler approach does not require a traversing system, but a mapping transformation is required to adjust the scanned contours of the molded rubber in a flexed condition to the blade surface in the rigid condition. In addition, severe tip erosion cannot be molded in the same way as surface dimples or scratches.

The 16 inch propeller was run extensively in severe cavitation conditions to look at analysis techniques, but the Keyence 2D sensor was not available for scanning this propeller before starting the test. To gain experience with the sensor, it was used to scan a ReproRubber mold of erosion damage on another propeller, and those results are shown in Figure 18.

RESULTS AND DISCUSSION

Wake Field Survey

LDV surveys were performed at 4 axial locations downstream of the wake generating strut for tunnel velocities of 10, 20, and 30 ft/sec (3, 6, and 9 m/sec) as measured by the Pitot-static probe.

These surveys were taken with a fairwater and dummy hub in place of the propeller. Vertical profiles (Y-positive up, Z-positive downstream) of the wake for all 4 axial locations at a tunnel velocity of 30 ft/sec (9 m/sec) are shown for the center of the wake in Figure 8 and for the propeller tip region of the wake in Figure 9. A full plane survey of the measured velocities 0.65 inches (16.5 mm) downstream of the foil is shown in Figure 10 as a contour plot. An outline of the propeller blade has been added to show where the wake falls on the blade.

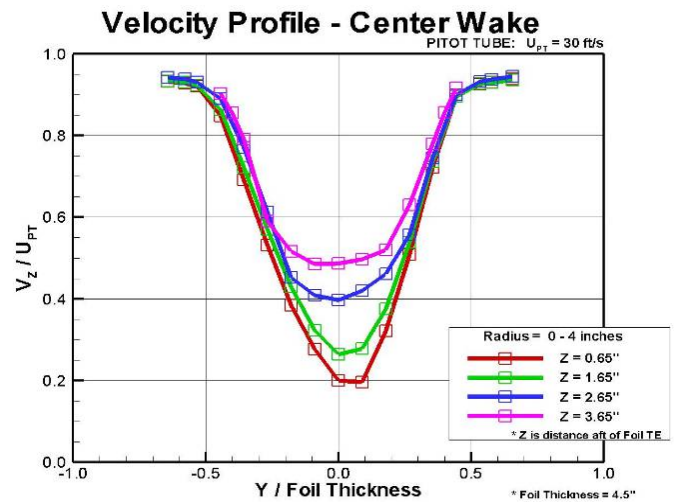


Figure 8: LDV Wake Survey - Center Wake Velocity Profile

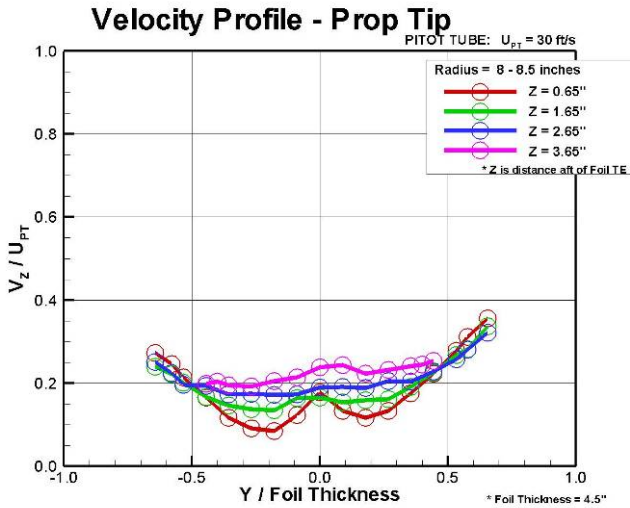


Figure 9: LDV Wake Survey - Outer Wake Velocity Profile

Figure 8 shows a wake deficit of as much as 80% and a thickness close to the strut thickness (4.5 inches, 114.3 mm) at the prop center. These are good conditions for mid-blade cavitation collapse. However, Figure 9 and Figure 10 also show a large, wide wake deficit ($0.1 V_z/U_{pt}$) out at the tip region of the 16 inch propeller. This large deficit is essentially a wall effect caused by the junction of the 24 inch VPWT contraction nozzle with the wake generation strut and the sudden entry of the flow into the open test section.

Cavitation Conditions

With the wake generating strut upstream of the propeller it became possible to observe extreme cavitation conditions on the propeller blades as they passed through the horizontal wake. By controlling tunnel velocity, tunnel static pressure, and propeller rpm, different cavitation conditions were achieved for different aspects of testing. A summary of the conditions can be found in Table 1.

Initial plans had been to run the 16 inch propeller at abnormally high load (low J) conditions and force severe leading edge sheet cavitation to occur along the blade. With a design J near 0.90, the propeller was run at J = 0.50 conditions. But the most severe cavitation occurred at the propeller tip because of the larger wake deficit in the wake outer edge. This created a problem for generating cavitation collapse on the mid-blade of the propeller. For most conditions, the leading edge suction side cavitation rolled up into the large tip vortex to form a continuous cavity, and the cavity collapsed on the propeller tip or beyond, missing the blade mid-chord region.

To isolate the leading edge cavity from the tip vortex, the propeller was run in a J range of 0.9 to 1.1. These conditions created leading edge cavities that collapsed near 2/3 chord at a sigma of 1.6

For the 12 inch propeller, a reduction in the tip vortex cavitation was observed, though not enough to be able to suppress the tip vortex completely and have only leading edge suction side cavitation. Further tests with this propeller were abandoned.

For 16 inch propeller stencil ink testing, imaging, and erosion damage, higher tunnel velocities (30 to 40 fps) and tunnel pressures near a half atmosphere resulted in the most favorable cavitation. At these conditions, the leading edge cavitation and the tip vortex mainly remained separated and the leading edge cavitation tended to collapse on the middle of the blade. However, even in these conditions, the tip vortex dominated the total cavitation volume.

For the accelerometer measurements, conditions were established that varied in magnitude, amount, and type of cavitation present. This was to determine if the accelerometers could be used to distinguish cavitation types as well as determine threshold levels for cavitation erosion damage.

The advance coefficient J and cavitation number σ are used in Table 1 to identify the different conditions. These parameters are defined as follows:

$$J = \frac{U_{pt}}{nD} \quad \sigma = \frac{P_s - P_v}{\frac{1}{2} \rho U_{pt}^2}$$

Where U_{pt} is the Pitot-static probe velocity, n is the propeller rpm, D is propeller diameter, P_s is tunnel static pressure, P_v is vapor pressure and ρ is water density.

Table 1: 24 inch VPWT Condition Summary

Condition	U_{pt} (ft/s)	J	σ	Figure
16 inch Prop	38.9	1.09	1.02	Figure 12
12 inch Prop	36.2	0.99	1.18	Figure 13
High Speed	29.3	0.91	1.75	Figure 14
Accel Cond 1	29.5	1.00	2.41	Figure 15&16
Accel Cond 2	29.7	1.24	2.37	Figure 16
Accel Cond 3	12.2	0.92	14.02	Figure 16
Accel Cond 4	29.6	1.33	2.40	Figure 16

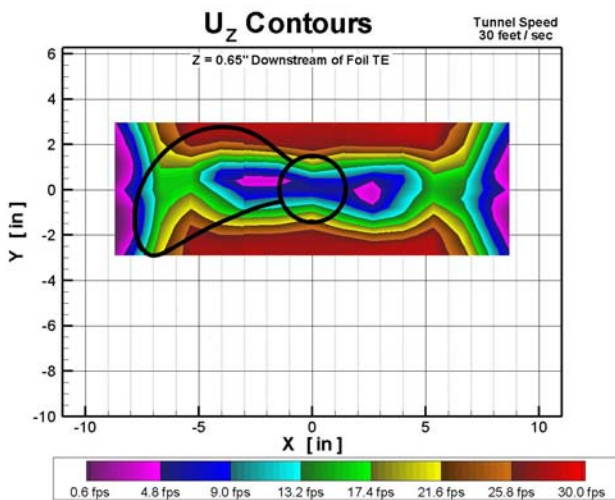


Figure 10: LDV Wake Survey - Velocity Field 0.65 inches downstream of the strut

Erosion Pattern Imaging

The 16 inch propeller was painted with stencil ink. Two of the blades were painted with brush-on ink, two with spray-on ink, and one blade was left unpainted. Comparing the blades with different ink would highlight differences in the ink

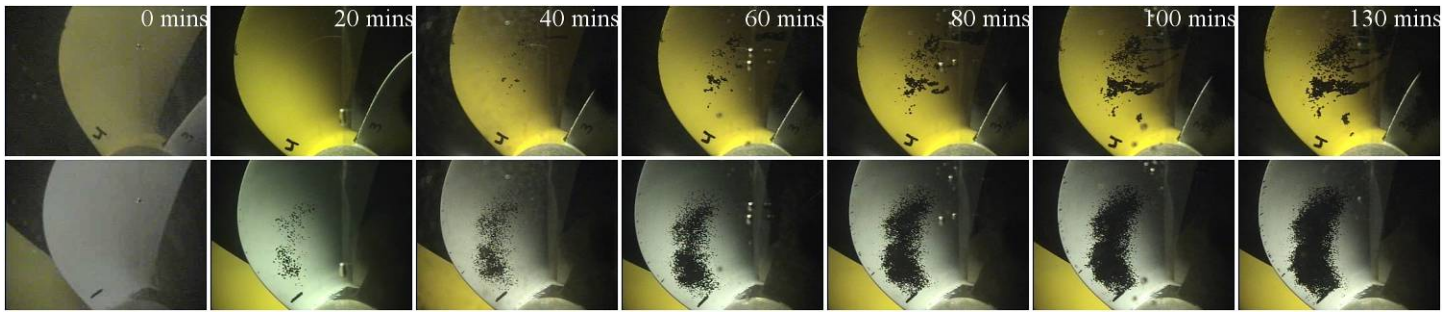


Figure 11: Stencil Ink Erosion Pattern, spray-on ink above, brush-on ink below

removal, and comparisons of the two blades with the same ink would indicate repeatability. The brush-on ink did not adhere to the blades or cover them as uniformly as the spray-on ink, and initial impressions were that the spray-on would show more uniform performance overall. The propeller was then run with for 130 minutes at an advance coefficient $J = 0.91$ and cavitation number $\sigma = 1.75$. The submersible camera was used to image the propeller blades at different times in the run. Sequential images of one brush-on and one spray-on blade are shown in Figure 11. The spray-on ink was not removed as easily and peeled off of places where cavitation collapse was not occurring. The brush-on ink patterns were almost identical between those two blades and the trend of ink removal with time was more consistent than with the spray-on ink.

The brush-on stencil ink was also a good indicator of the location where cavitation erosion would eventually occur. When the propeller was run at this same condition for a longer time, pits of material were removed (see Figure 17) that matched the stencil ink removal pattern. As has been shown in previous studies [7], stencil ink is a good indicator of existence and location of future cavitation erosion damage.

Although a spray-on ink may apply more uniformly and more easily than a brush-on ink, the removal by cavitation may not be as repeatable and peeling can occur.

The best still images of the propeller and cavitation were made with the high resolution imaging system using the strobe lights for illumination. This imaging method also proved useful for studying the unsteadiness of the cavitation conditions. Because each frame in a time sequence is a snap shot of the cavitation on the same blade at different rotations, changes of the cavity pattern from rotation to rotation become clear. Typically in this test, the unsteadiness in cavitation appeared as fluctuations in cavity area and volume as well as intermittency of a collapse event in the mid-blade region. This unsteady behavior could be attributed to turbulent inflow conditions from the wake generator. Snap shots of cavitation on the 16 inch and 12 inch propellers from the high resolution imaging system are shown in Figure 12 and Figure 13.

The high speed imaging system used in this test provided insight into the underlying structure of the cavitation and observation of the cavitation collapse phenomenon. Additionally, without high speed imaging it would have been nearly impossible to observe the interaction between the leading edge cavitation and the tip vortex.

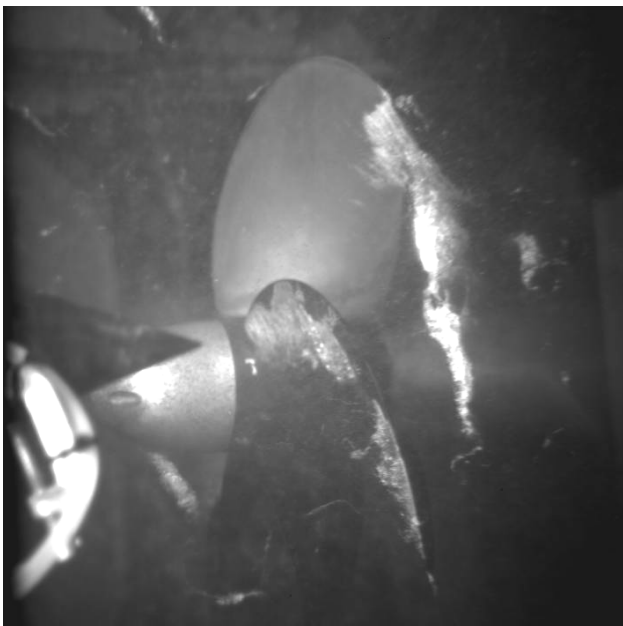


Figure 12: High resolution image of the 16 inch propeller ($J=1.09$, $\sigma=1.03$)

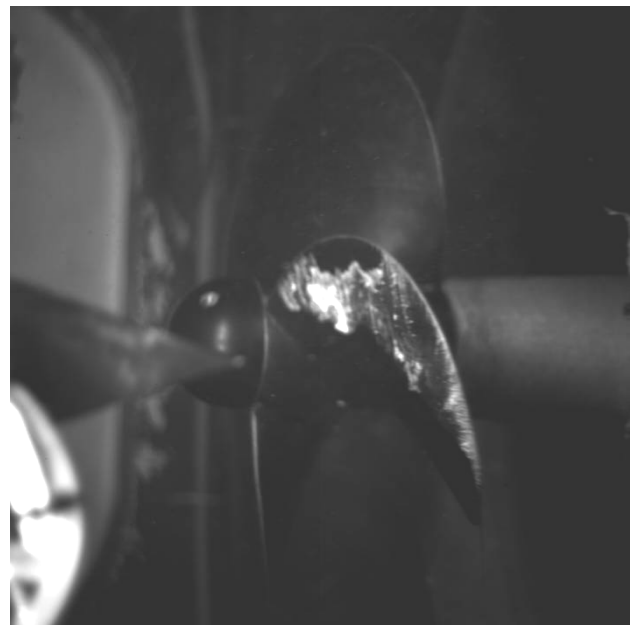


Figure 13: High Resolution image of the 12 inch propeller ($J=0.99$ and $\sigma=1.18$)

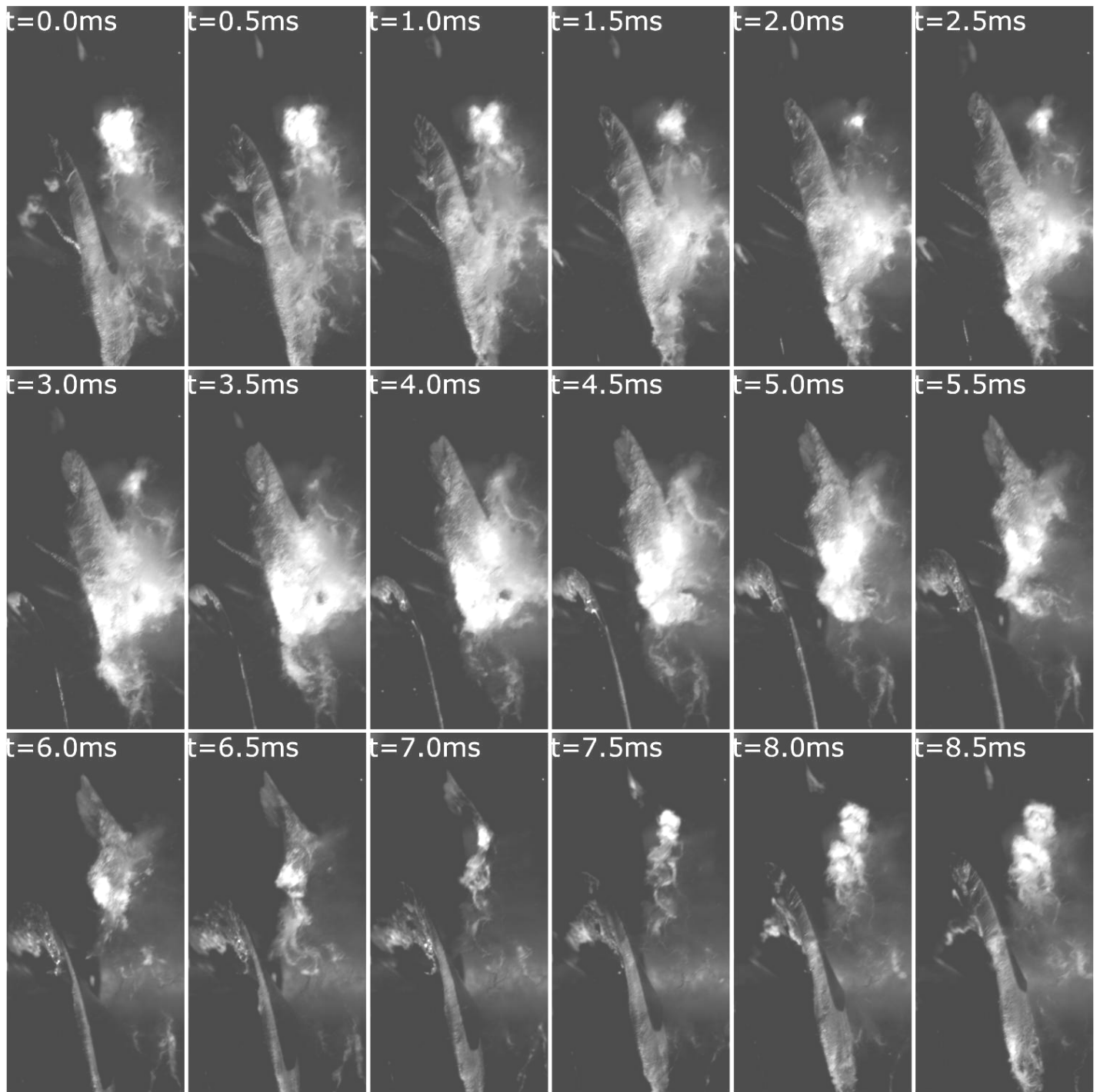


Figure 14: High Speed Image Sequence of Tip Vortex Cavitation

The tip vortex cavitation, while undesirable for the erosion quantification, did provide an interesting cavitation event to observe at high speed. Figure 14 is a frame sequence of a tip vortex generation and collapse as a blade passes through the foil wake (from bottom to top of the frame). From $t=6.5$ ms to $t=8.0$ ms the tip vortex cavity collapses toward the tip and a resulting cloud can be observed from the impact of the collapse with the tip of the propeller blade. This event generated the most extreme cavitation erosion damage to the propeller.

Acoustic Emission

The 0.2 second samples acquired from the 3 accelerometers mounted in the 24 inch VPWT were recorded at the 4 operating conditions indicated in Table 1. The 500 kHz time series samples of 0.2 seconds long were digitally high-pass filtered at 50 kHz to remove low frequency content. Figure 15 shows a sample filtered time-series of data acquired from the accelerometer mounted on 24 inch VPWT capture nozzle. The bursts in the accelerometer time series are associated with cavitation collapse events.

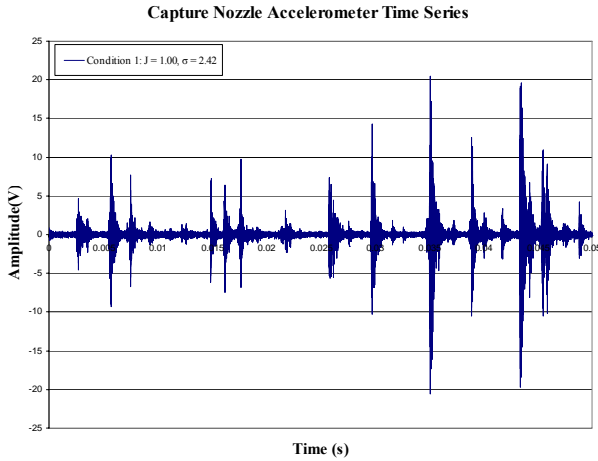


Figure 15: Accelerometer Time-Series

The un-filtered time series samples were also processed using peak-hold analysis. This involved taking the maximum amplitude (in dB) of each 244 μ s window of the 500 kHz time series. The amplitude for this calculation is defined as follows:

$$A = 10 \times \log \left(\frac{V_s}{V_f} \right)^2$$

In which V_s is sample voltage and V_f is a reference voltage (1 mV was used for this analysis).

The peak-hold data were plotted as a histogram showing the frequency of occurrence of amplitudes over the 0.2 second time series. By analyzing the peak in this histogram, threshold levels for different cavitation conditions can be compared. Peak hold histograms for the 4 accelerometer cavitation conditions are shown in Figure 16 for the downstream strut accelerometer.

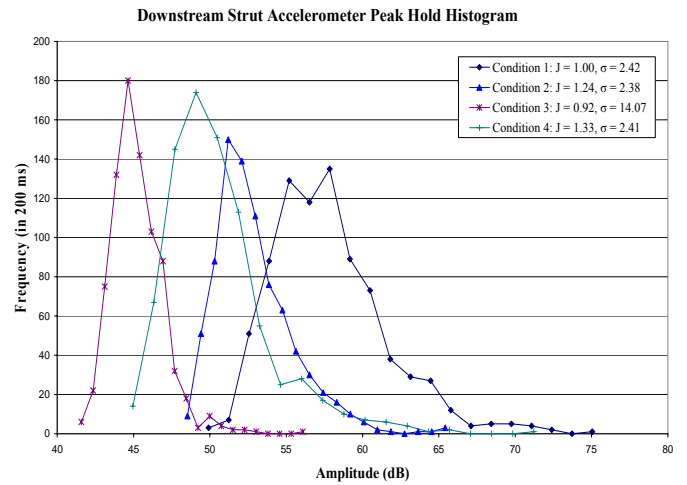


Figure 16: Accelerometer Peak-Hold Histogram

The different cavitation conditions can be clearly distinguished by the different positions and shapes of the peaks. Condition 1 had the highest intensity cavitation and consisted of tip vortex and suction side leading edge cavitation forms. Conditions 2 and 4 were similar with both tip vortex cavitation and pressure side leading edge cavitation. However, condition 2 had a more pronounced tip vortex, appearing as a higher amplitude peak, while condition 4 had more pressure side cavitation. Condition 3 was a low intensity condition with only tip vortex cavitation present.

Erosion Damage Evaluation

The resulting damage of the 16 inch propeller from extensive operation at extreme cavitation conditions is shown in Figure 17. The most damage occurred at the tip. However, removal of the propeller anodization matching the stencil ink removal pattern on the mid-blade area is seen in Figure 11. This



Figure 17: Cavitation Erosion Damage

is attributed to leading edge suction side cavitation

The measurement and analysis of cavitation erosion damage with ReProRubber molds and the Keyence sensor has not yet been completed. However, a rubber mold of erosion damage on an existing prop damaged in a previous test was scanned with the Keyence sensor and the results are shown in Figure 18.

Summary

Initial tests to model cavitation erosion on a propeller and develop analysis and measurement techniques have been completed. Creation of pure leading edge suction side cavitation with trailing edge collapse on the blade is difficult because of interactions with the tip vortex cavity. Although this test setup accentuated this problem because of the proximity of the propeller tip to the wall, strut-based wakes that extend across the propeller disc will generally have this problem. Using the wake generator to house an upstream camera offers a clear, normal view of the blade cavitation, and mounting a mirror in the same open channel allows optical access with the same view but from external cameras. Strobe lighting synchronization offers the best illumination for normal video cameras and multiple incandescent lights may be required for high speed imaging. Brush on stencil inks can be good indicators of cavitation erosion and the uniformity of the applied ink does not severely affect its removal. Intensity and frequency of accelerometer impact peaks are different for different cavitation types. Linear scanning techniques can be applied to measure the volume of eroded material, but its final application to full propeller scans has not been demonstrated.

Acknowledgements

The authors would like to acknowledge the sponsors of this project, Ki-Han Kim, Program Manager, Office of Naval Research and Brian Cavett, Program Manager, Quick Reaction Fund, OUSD (AT&L) ODDR&E/Plans and Programs.

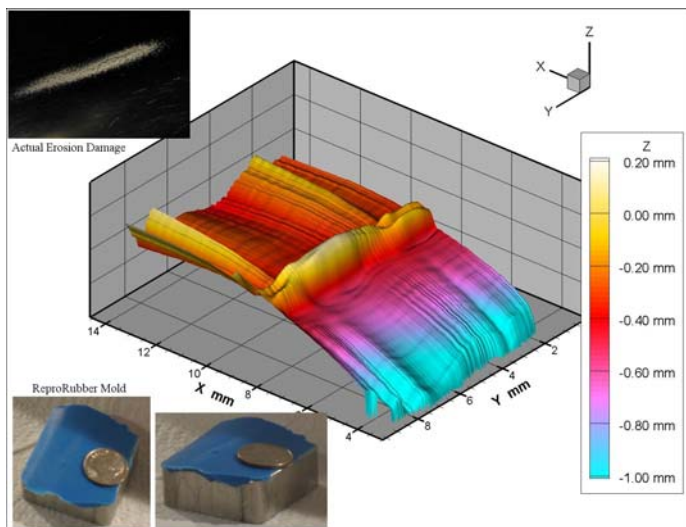


Figure 18: Erosion Damage, ReProRubber Mold, and Scan Results

References

- [1] Bachert, B., Ludwig, G., Stoffel, B., and Baumgarten, S., "Comparison of Different Methods for the Evaluation of Cavitation Damaged Surfaces", *Proceedings of ASME Fluids Engineering Division Summer Meeting*, 553-559, June 2005.
- [2] Bark, G., Berchiche, N., and Grekula, M., *Application of Principles for Observation and Analysis of Eroding Cavitation – The EROCAV Observation Handbook*, Department of naval Architecture and Ocean Engineering, Chalmers University of Technology, Göteborg, Sweden, 2004.
- [3] Chesnakas, C. J., and Jessup, S. D., "Tip-Vortex Induced Cavitation on a Ducted Propulsor", *Proceedings of ASME Fluids Engineering Division Summer Meeting*, July 2003.
- [4] Collins, S., Williams, P., "Low-Temperature Colossal Supersaturation", *Advanced Materials and Processes*, September 2006.
- [5] Dahmer, D., and Miller, M., "The Effect of Blade Erosion of Injecting Air Ahead of a Cavitating Propeller", *David W. Taylor Naval Ship Research and Development Center Report*, March 1980.
- [6] Flexbar Corporation, Long Island, NY, USA <http://www.flexbar.com>
- [7] ITTC Recommended Guidelines and Procedures, Propulsion; Cavitation Induced Erosion on Propellers, Rudders and Appendages Model Scale Experiments, 7.5-02-03-03.5, itc.sname.org
- [8] Jessup, S. D., "Viscous Aspects of Propeller Flows", PH.D. Thesis, Catholic University of America, 1989.
- [9] Keyence Corporation, Osaka, Japan, <http://www.keyence.com>
- [10] Lichtman, J. Z., and Weingram, E. R., "The Use of a Rotating Disk Apparatus in Determining Cavitation Erosion Resistance of Materials", *ASME Symposium on Cavitation Research Facilities and Techniques*, 185-196, May 1964.
- [11] Miller, M., "The Effect of Some Propeller and Wake Characteristics on Cavitation Erosion", *David W. Taylor Naval Ship Research and Development Center Report*, April 1980.
- [12] Moeny, M., Weldon, M., Stinebring, D., Straka, W., and Pierzga, M., "Cavitation Damage from and Induced Secondary Vortex", *Proceedings of ASME Fluids Engineering Division Summer Meeting*, August 2008.
- [13] Tash, H. A., Sadeghi, M., Tabar, M. T. S., and Etefagh, M. M., "Cavitation Intensity Measurement by Analysis of Pump Structure Oscillation – A New Parametric Approach", *Proceedings of ASME Fluids Engineering Division Summer Meeting*, August 2008.